International Journal of Engineering Research & Technology (IJERT)
ISSN: 2278-0181
Vol. 6 Issue 12, December - 2017

Acoustic Model of a Duct with a Varying Cross - Sectional Area and a Non - zero Mean Flow

Myung-Gon Yoon
Department of Precision Mechanical Eng.
Gangneung - Wonju National University
Wonju 26403, Republic of Korea

***Abstract*—In this paper we propose a semi-analytic one-dimensional acoustic model of a duct which has a continuously varying cross-sectional area under the non-zero mean flow condition. Our idea is to approximate the region of varying area as a sequence of abrupt area change. It is shown that the commonly employed approximation method in which the area varying zone is replaced with one abrupt area change can result in significant errors in terms of acoustic transfer matrix.**

***Keywords*—One-dimensional acoustic model, Acoustic Transfer Matrix**

I. Introduction

A precise acoustic model of a duct with a continuously varying cross-sectional area, such as the interval $[x_1, x_2]$ in an acoustic model of a gas turbine engines in Fig. 1, is a difficult task. The acoustic model of the area contracting part $[x_1, x_2]$ should represent physical behaviors but at the same time it need be mathematically simple and explicit to be integrated for an acoustic analysis of the whole system.

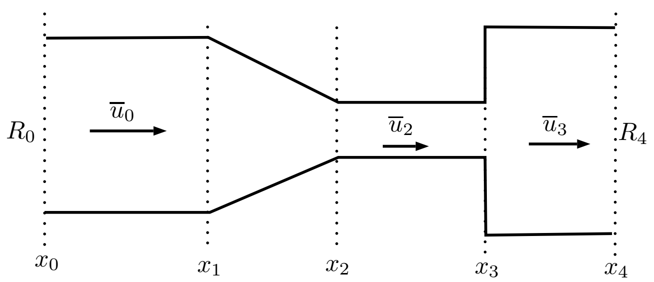

Fig. 1: A simple acoustic model of gas turbine

Some results exist in literature for the cases when there is no mean flow and the area contraction over the interval $[x_1, x_2]$ is not significant [1]. In addition, some recent results can handle more general cases but the model is too complicated and implicit, e.g. see [2], [3].

An intuitively appealing and commonly used approach in practice is to approximate the area varying region $[x_1, x_2]$ as having an abrupt area change at $x_e \in [x_1, x_2]$ as depicted in Fig. 2. This approach can be naturally generalised to introduce a sequence of tiny area jumps as shown in Fig. 3 instead of one.

A fundamental question is whether or not the acoustic model corresponding to n-jump approximation converges to a certain model in an appropriate sense as the number of jumps n increases. In addition, assuming that the many-jump model converges, our next question is whether or not it is possible to cleverly choose the fictitious area jump position x_e in Fig. 2 of the single jump model such a way that the associated model can be reasonably close to multi-step model. These two questions are investigated in this paper.

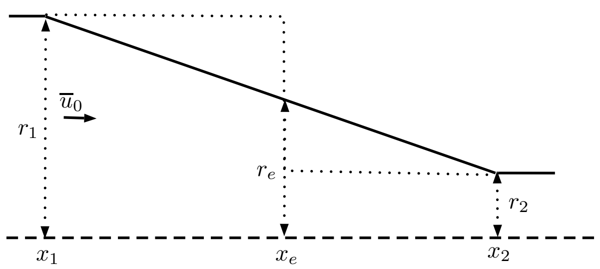

Fig. 2: Single step approximation

International Journal of Engineering Research & Technology (IJERT)
ISSN: 2278-0181
Vol. 6 Issue 12, December - 2017

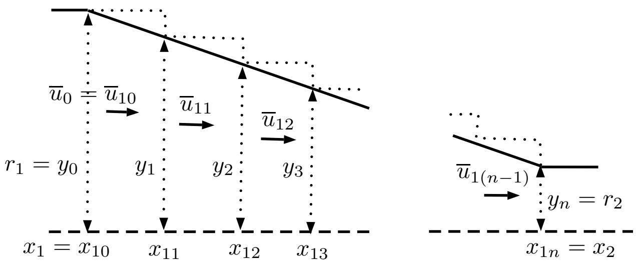

Fig. 3: Mutiple jump approximation

II. Acoustic Model

A. Single step model

In one-dimensional acoustic model of a duct in Fig. 2, we need to characterize the relations between pressure and volume velocity perturbations between x_1 and x_2.

For the intervals $[x_1, x_e)$ and $(x_e, x_2]$, acoustic waves simply propagate over a duct of a constant area and thus it follows that

$$\begin{bmatrix} p' \\ \overline{\rho} c u' \end{bmatrix}_{x_e} = \frac{1}{2} \begin{bmatrix} e^{-\tau_1^+ s} + e^{\tau_1^- s} & e^{-\tau_1^+ s} - e^{\tau_1^- s} \\ e^{-\tau_1^+ s} - e^{\tau_1^- s} & e^{-\tau_1^+ s} + e^{\tau_1^- s} \end{bmatrix} \begin{bmatrix} p' \\ \overline{\rho} c u' \end{bmatrix}_{x_1} \tag{1}$$

where the superscript $'$ and over-line denote perturbation and mean value, respectively. Moreover ρ and c denote density and sound speed and

$$\tau_1^{\pm} = \frac{x_e - x_1}{c \pm \overline{u}_0} \tag{2}$$

Similarly we have

$$\begin{bmatrix} p' \\ \overline{\rho} c u' \end{bmatrix}_{x_2} = \frac{1}{2} \begin{bmatrix} e^{-\tau_2^+ s} + e^{\tau_2^- s} & e^{-\tau_2^+ s} - e^{\tau_2^- s} \\ e^{-\tau_2^+ s} - e^{\tau_2^- s} & e^{-\tau_2^+ s} + e^{\tau_2^- s} \end{bmatrix} \begin{bmatrix} p' \\ \overline{\rho} c u' \end{bmatrix}_{x_e} \tag{3}$$

, $\tau_2^{\pm} = (x_2 - x_e)/(c \pm \overline{u}_1)$, $\overline{u}_1 = \overline{u}_0/\beta$ and $\beta = (r_2/r_1)^2$ denotes the area ratio.

At the point of abrupt area change x_e, it holds that

$$\begin{bmatrix} p' \\ \overline{\rho} c u' \end{bmatrix}_{x_{e+}} = \begin{bmatrix} 1 & \xi(\beta) M_1 \\ 0 & 1/\beta \end{bmatrix} \begin{bmatrix} p' \\ \overline{\rho} c u' \end{bmatrix}_{x_{e-}} \tag{4}$$

$$\xi(\beta) = \frac{-2 + 3\beta^2 - \beta^3}{2\beta^2} \tag{5}$$

which follows from the continuity condition and the stagnation pressure loss across the area jump [4].

A combination of the results (1), (3) and (4) gives

$$\begin{bmatrix} p' \\ \overline{\rho} c u' \end{bmatrix}_{x_2} = S(\alpha, s) \begin{bmatrix} p' \\ \overline{\rho} c u' \end{bmatrix}_{x_1} \tag{6}$$

$$S(\alpha, s) := \begin{bmatrix} S_{11}(\alpha, s) & S_{12}(\alpha, s) \\ S_{21}(\alpha, s) & S_{22}(\alpha, s) \end{bmatrix} \tag{7}$$

where $0 \leq \alpha \leq 1$ denotes the relative location of area jump defined

$$\alpha := \frac{x_e - x_1}{x_2 - x_1}. \tag{8}$$

B. Multiple step model

We divide the interval $[x_1, x_2]$ into n sub-intervals $[x_{1(k-1)}, x_{1k})]$ for $k = 1, \cdots, n$ where $x_1 = x_{10}$ and $x_{1n} = x_2$ as shown in Fig. 3. Each sub-interval is composed of a wave propagation for a distance $\Delta := (x_2 - x_1)/n$ and then a sudden area contraction. This can be written as

$$\begin{bmatrix} p' \\ \nu' \end{bmatrix}_{x_{1k}} = T_{k-1}^k \begin{bmatrix} p' \\ \nu' \end{bmatrix}_{x_{1(k-1)}} \quad (k = 1, \cdots, n) \tag{9}$$

where the transfer matrix T_{k-1}^k between sub-elements is given

$$T_{k-1}^k := \frac{1}{2} \begin{bmatrix} 1 & \xi(\beta_{1k}) \overline{u}_{1(k-1)}/c_1 \\ 0 & 1/\beta_{1k} \end{bmatrix} \begin{bmatrix} e^{-\tau_{1k}^+} + e^{\tau_{1k}^-} & e^{-\tau_{1k}^+} - e^{\tau_{1k}^-} \\ e^{-\tau_{1k}^+} - e^{\tau_{1k}^-} & e^{-\tau_{1k}^+} + e^{\tau_{1k}^-} \end{bmatrix} \tag{10}$$

$$\beta_{1k} := \frac{y_k^2}{y_{k-1}^2} = \left(\frac{k(r_2/r_1 - 1) + n}{(k-1)(r_2/r_1 - 1) + n} \right)^2 \tag{11}$$

$$\overline{u}_{1k} := \overline{u}_{1(k-1)}/\beta_{1k} = \overline{u}_1 / \prod_{i=1}^{k} \beta_i \tag{12}$$

$$\tau_{1k}^{\pm} := \frac{(x_2 - x_1)/n}{c_1 \pm \overline{u}_{1(k-1)}} \tag{13}$$

Form a sequential application of the above transfer matrix for sub-intervals, the transfer matrix of the area varying interval $[x_1, x_2]$ can be explicitly written as

$$\begin{bmatrix} p' \\ \nu' \end{bmatrix}_{x_2} = M(n, s) \begin{bmatrix} p' \\ \nu' \end{bmatrix}_{x_1}$$

$$M(n, s) = \prod_{k=1}^{n} T_{k-1}^k := \begin{bmatrix} M_{11}(n, s) & M_{12}(n, s) \\ M_{21}(n, s) & M_{22}(n, s) \end{bmatrix}. \tag{14}$$

International Journal of Engineering Research & Technology (IJERT)
ISSN: 2278-0181
Vol. 6 Issue 12, December - 2017

III. A Numerical Case Study

The following parameters were chosen for a numerical case study ;

$$L = x_2 - x_1 = 60, \; r_1 = 32.5, \; r_2 = 10.6 \qquad (15)$$

in [milli-meter] unit and $c = 345$ [meter/sec].

A. Model Convergence

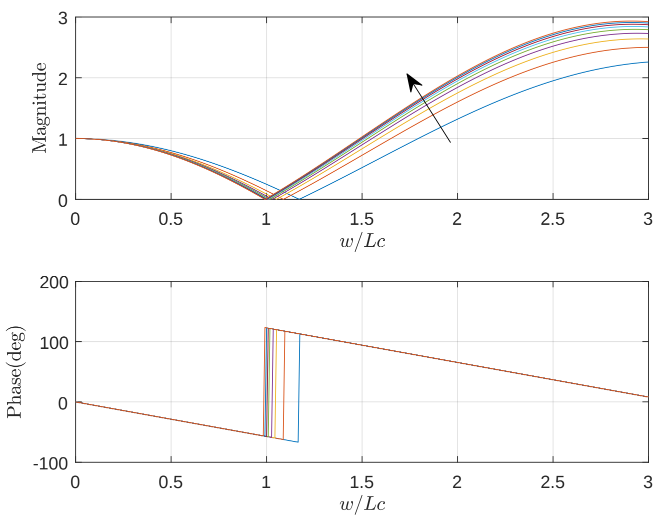

Fig. 4: Bode plot of $M_{11}(n,s)$ with $n \in [2,10]$ and $\overline{u}_1 = 0$

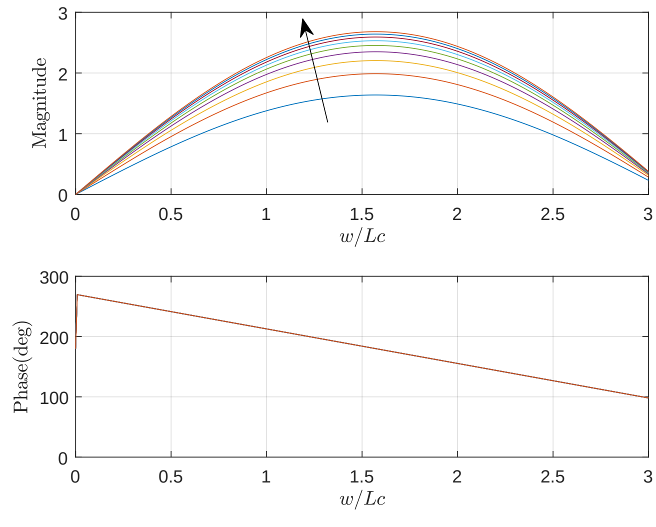

Fig. 5: Bode plot of $M_{12}(n,s)$ for $n \in [2,10]$ and $\overline{u}_1 = 0$

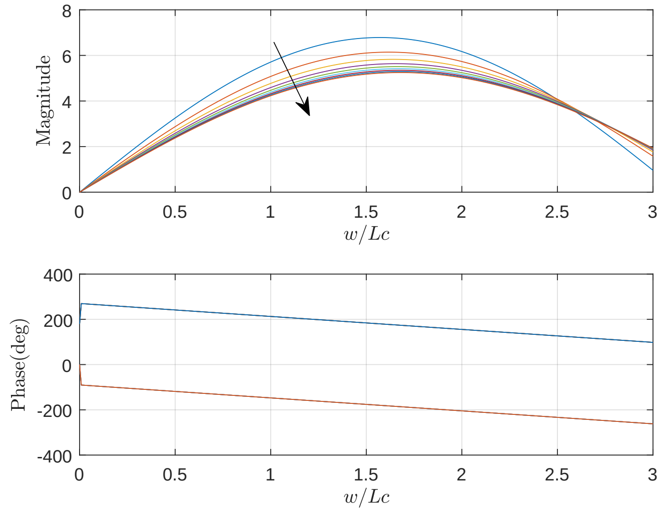

Fig. 6: Bode plot of $M_{21}(n,s)$ for $n \in [2,10]$ and $\overline{u}_1 = 0$

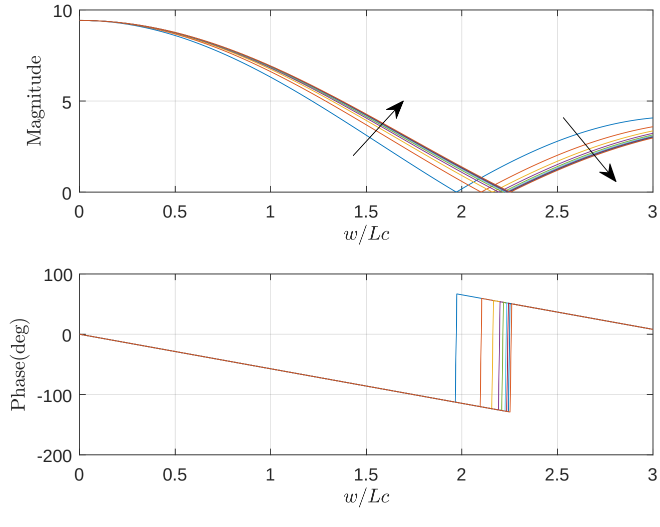

Fig. 7: Bode plot of $M_{22}(n,s)$ for $n \in [2,10]$ and $\overline{u}_1 = 0$

We have computed the Bode plots of four component $M_{ij}(n,s)$ of the acoustic transfer matrix in (14). The horizontal axis in Fig. 4-7 denotes the normalized frequency w/Lc $(w = 2\pi f)$, $L = x_2 - x_1$ and the arrows indicates the direction of increasing $n \in [2,10]$.

The overall results strongly suggests that the multiple step model quickly converges to a limit model as the number of steps increases.

International Journal of Engineering Research & Technology (IJERT)
ISSN: 2278-0181
Vol. 6 Issue 12, December - 2017

B. Resonance frequency shift

The anti-resonance frequency around $w/Lc \approx 1$ in Fig. 4 was zoomed with a larger $n \in [5, 30]$ in Fig. 8. An interesting observation here is that, as n increases, the anti-resonance frequency slightly decreases toward $w/Lc = 0.968$ roughly. Another way of looking at this result is that the area variation gave rise to an increased duct length $L \to L/0.968 = 1.03L$ (3%) effectively.

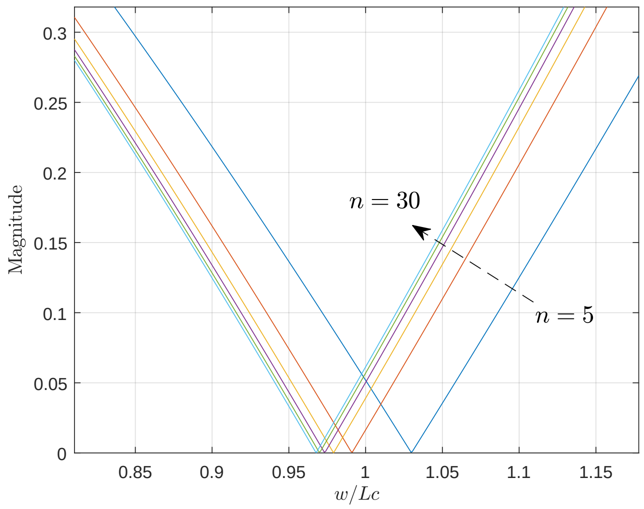

Fig. 8: First anti-resonance frequency of $M_{11}(n, s)$ on $n \in [5, 30]$ and $\overline{u}_1 = 0$

C. Mean flow effect

One of the most surprising result in this paper is that the acoustic transfer matrix significantly depends on mean flow.

One can see this clearly in the Bode magnitude plot of $M_{11}(n, s)$ (upper) and $M_{12}(n, s)$ (lower) in Fig. 9 where $n = 10$ and the Mach number $M_1 := \overline{u}_0/c \in [0, 0.02]$.

Note that the tiny mean flow $\overline{u}_0 = 6.9$ (meter/sec) of the case $M_1 = 0.02$ can virtually eliminate the anti-resonance peak around $w/Lc = 1$. Our computation revealed, but not included here, that the mean flow dependency however is less significant in the cases of another two components $M_{21}(n, s)$ and $M_{22}(n, s)$.

D. Dependency on jump position

Let us consider the next question; *Is it possible to cleverly choose a fictitious area jump position x_e of the one-jump model (7) such that the resulting model becomes similar to the multi-jump model (14) ?*

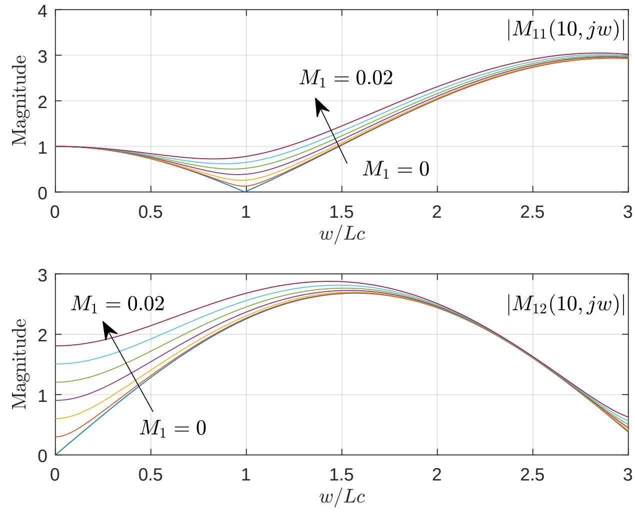

Fig. 9: Bode magnitude plots of $|M_{11}(n, jw)|$ and $|M_{12}(n, jw)|$ with mean flow $M_1 \in [0, 0.02]$

Seeking an answer to this question, we have compared the Bode plot of $S(\alpha, s)$ with $M(10, s)$ in Fig, 10-13 with a zero-mean flow. The **thick** cyan lines in those figures denote the Bode plot of $M(10, s)$.

An interesting fact is that, in the case of $\{S_{11}, S_{22}\}$ shown in Fig. 10 and Fig. 13, both α and $1 - \alpha$ give the same results.

Note from Fig. 10 that either a small $\alpha = 0.1$ or a large $\alpha = 0.9$ results in $S_{11}(\alpha, s)$ close to $M_{11}(10, s)$. In contrast, in other three cases in Fig. 11-13, the single step model becomes similar to multiple step model with a moderate choice $\alpha \approx 0.5$ in overall.

These observation suggest that the single step model is an intrinsically different from the multiple step model and thus it is an inaccurate acoustic model, irrespectively of how to choose a step location.

IV. Conclusion

We developed a semi-analytic one-dimensional acoustic model of a duct with a continuously varying cross-sectional area under the non-zero mean flow condition. Our numerical case study suggests that the acoustic transfer matrix of a multiple step approximation for

International Journal of Engineering Research & Technology (IJERT)
ISSN: 2278-0181
Vol. 6 Issue 12, December - 2017

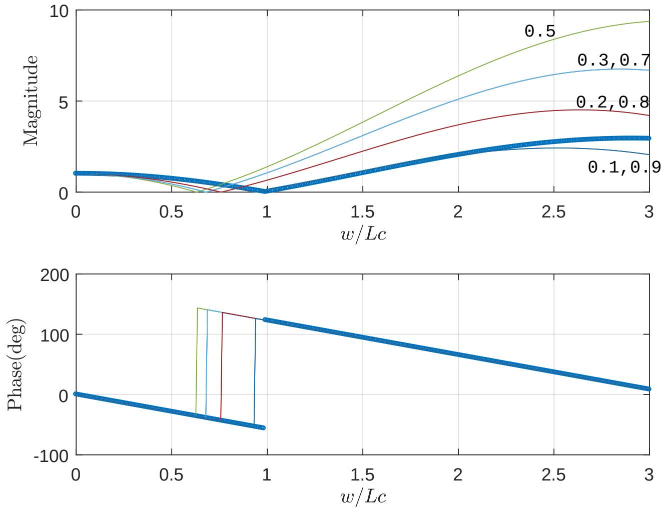

Fig. 10: Bode plot of $\{M_{11}(10, s), S_{11}(\alpha, s)\}$

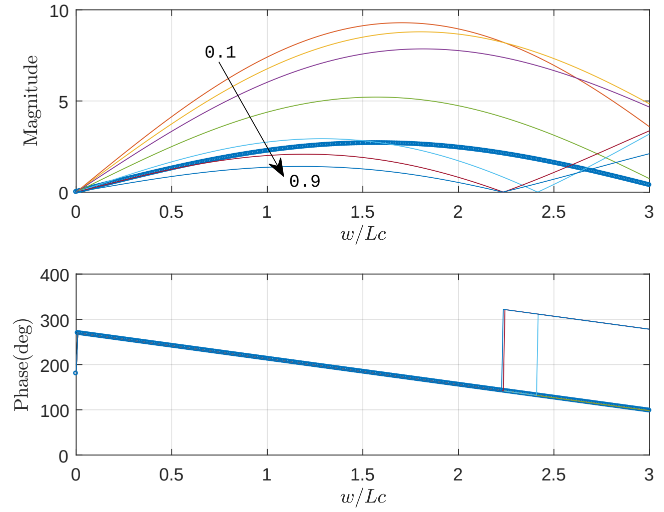

Fig. 11: Bode plot of $\{M_{12}(10, s), S_{11}(\alpha, s)\}$

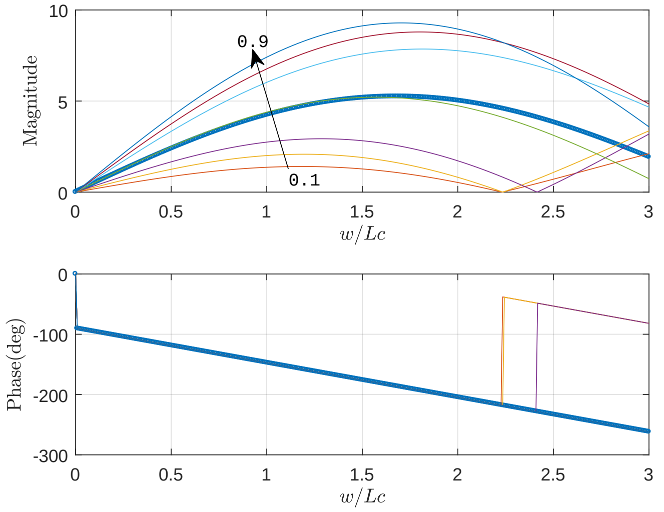

Fig. 12: Bode plot of $\{M_{21}(10, s), S_{11}(\alpha, s)\}$

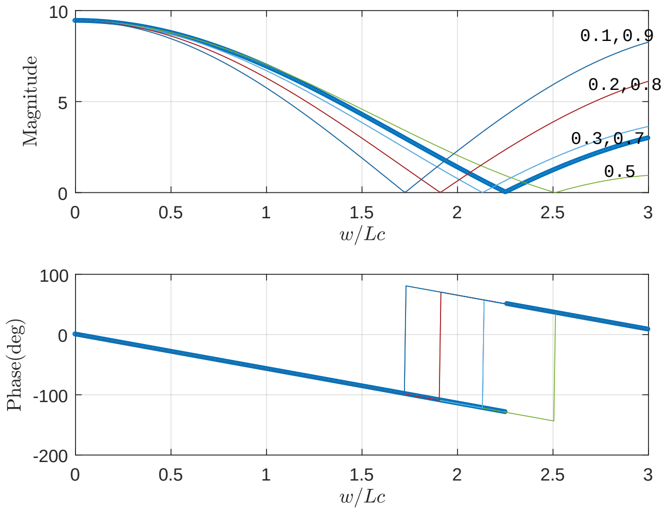

Fig. 13: Bode plot of $\{M_{22}(10, s), S_{11}(\alpha, s)\}$

the varying cross-sectional region converges to a limit matrix as the number of steps increases. In addition, it was found that a single step model is an erroneous approximation irrespectively of the choice of a step location.

REFERENCES

[1] R. D. Ayers, L. J. Eliason, and D. Mahgerefteh, "The conical bore in musical acoustics," *American Journal of Physics*, vol. 53, no. 6, pp. 528–537, 1985.
[2] Q. Min, W. He, J. T. Q. Wang, and Q. Zhang, "A study of stepped acoustic resonator with transfer matrix method," *Acoustical Physics*, vol. 60, no. 4, pp. 492–498, 2014.
[3] A. Gentemann, A. Fischer, S. Evesque, and W. Polifke, "Acoustic transfer matrix reconstruction and analysis for ducts with sudden change of area," in *9th AIAA/CEAS Aeroacoustics Conference and Exhibit*, 2003.
[4] M. L. Munjal, *Acoustics of Ducts and Mufflers*, 2nd ed. Wiley, 2014.